Biosensors and Bioelectronics 49 (2013) 512–518

Contents lists available at SciVerse ScienceDirect

Biosensors and Bioelectronics

journal homepage: www.elsevier.com/locate/bios

A new type of glucose biosensor based on surface acoustic wave resonator using Mn-doped ZnO multilayer structure

Jingting Luo [a,*], Pingxiang Luo [b], Min Xie [b], Ke Du [c], Bixia Zhao [c], Feng Pan [d,**], Ping Fan [a], Fei Zeng [d], Dongping Zhang [a], Zhuanghao Zheng [a], Guangxing Liang [a]

[a] Institute of Thin Film Physics and Applications, Shenzhen Key Laboratory of Sensor Technology, Shenzhen University, Shenzhen 518060, China
[b] Maternity and Child Care Centers in Fujian Province, Fuzhou 350001, China
[c] Affiliated Nanhua Hospital of University of South China, Hunan 421002, China
[d] Laboratory of Advanced Materials, Department of Materials Science and Engineering, Tsinghua University, Beijing 100084, China

ARTICLE INFO

Article history:
Received 27 February 2013
Received in revised form
28 April 2013
Accepted 20 May 2013
Available online 12 June 2013

Keywords:
Glucose
Surface acoustic wave (SAW)
ZnO
Glucose oxidase functional immobilization
Biosensor

ABSTRACT

This work reports a high-performance Mn-doped ZnO multilayer structure Love mode surface acoustic wave (SAW) biosensor for the detection of blood sugar. The biosensor was functionalized via immobilizing glucose oxidase onto a pH-sensitive polymer which was attached on Mn-doped ZnO biosensor. The fabricated SAW glucose biosensor is highly sensitive, accurate and fast with good anti-interference. The sensitivity of the SAW glucose biosensor is 7.184 MHz/mM and the accuracy is 6.96×10^{-3} mM, which is sensitive and accurate enough for glucose monitoring. A good degree of reversibility and stability of the glucose sensor is also demonstrated, which keeps a constant differential frequency shift up to 32 days. Concerning the time response to human serum, the glucose sensor shows a value of 4.6 ± 0.4 min when increasing glucose concentrations and 7.1 ± 0.6 min when decreasing, which is less than 10 min and reach the fast response requirement for medical applications. The Mn-doped ZnO Love mode SAW biosensor can be fully integrated with CMOS Si chips and developed as a portable, passive and wireless real time detection system for blood sugar monitoring in human serum.

1. Introduction

Diabetes has become a worldwide public health problem that affects more than 347 million people around the world (WHO, 2013) and causes an estimated 3.4 million deaths every year due to hypoglycemic and severe diabetic complications (Kottmann et al., 2012). Results from the diabetes care and complications trials show that frequent testing of blood sugar level and timely insulin administration are crucial to prevent diabetic complications (Shibata et al., 2010). Nowadays, millions of diabetics need to test their glucose every day and most of the testing system needs a drop of blood collection for each measurement. The pain and inconvenience of blood collection testing have led to poor patient acceptance of a tight control regimen, which causes the glucose testing performed rarely frequently enough to follow glucose dynamics. Fortunately, continuous glucose measurement is promising to solve the problem (Vashist, 2012). The continuous glucose monitoring system provides maximal information about floating glucose levels throughout the day, which not only alarms the danger of hypo- and hyperglycemia but also assists in adjusting the diet and medical treatment. Therefore, numerous efforts have been focused on the development of continuous glucose monitoring system during the last decades (Atanasov et al., 1997; Klueh et al., 2005; Boss et al., 2011; Vashist, 2012; Wang et al., 2013).

In the past few years, surface acoustic wave biosensors have been widely used in bioanalytical and biosensing field due to its advantages of highly sensitive, reliable and reusable for responding to various measurands (Gronewold, 2007; Jung et al., 2007; Laenge et al., 2008; Rocha-Gaso et al., 2009; Voiculescu and Nordin, 2012; Yan et al., 2012; Katardjiev and Yantchev, 2012; Di Pietrantonio et al., 2013). SAW devices are mass transducers that can be integrated into portable micro-array systems, making it cheap and suitable for medical application. The majority of these devices were fabricated on thick commercial piezoelectric substrates such as lithium niobate ($LiNbO_3$), lithium tantalate ($LiTaO_3$) and quartz. SAW biosensors on quartz suffer from low electromechanical coupling coefficients, high penetration depth, and low dielectric permittivity when working in a liquid media, while SAW biosensors on $LiNbO_3$ and $LiTaO_3$ suffer from the attenuation of the acoustic wave due to the excitation of bulk acoustic waves in the crystal (Krishnamoorthy et al., 2008).

Recently, ZnO piezoelectric film based SAW biosensor have gained attention (Fu et al., 2010; Arya et al., 2012; Voiculescu and

* Corresponding author. Tel.: +86 755 26538974; fax: +86 755 26538735.
** Corresponding author. Tel.: +86 10 62772907; fax: +86 10 62771160.
E-mail addresses: luojt@szu.edu.cn, luojt@hotmail.com (J. Luo), panf@mail.tsinghua.edu.cn (F. Pan).

0956-5663/$ - see front matter © 2013 Elsevier B.V. All rights reserved.
http://dx.doi.org/10.1016/j.bios.2013.05.021

Nordin, 2012). ZnO possesses strong piezoelectric nature and good biocompatibility. Furthermore, it can grow on SiO_2/Si and Si substrates with good quality, which offers the advantage of monolithic integration with the advanced complementary metal oxide semiconductor (CMOS) and microelectromechanical systems (MEMS) technology, providing the opportunity for full integration with read-out and signal processing circuitry (Krishnamoorthy et al., 2006, 2008; Voiculescu and Nordin, 2012). In many biodetection applications, the biosensor can be based on passive and wireless SAW devices with small size (Pohl, 2000; Lee et al., 2007). No direct physical connections to the sensor are needed, nor is any internal power source (i.e., battery) needed for sensor operation. Therefore, SAW biosensors are particularly suit for continuous detection with real-time patient evaluation. Moreover, SAW biosensor using ZnO piezoelectric film based multilayer structure can reach high working frequencies and large electromechanical coupling coefficient, which provides the enhanced sensitivity. This prompted us to develop ZnO piezoelectric film multilayer structure SAW biosensor targeting continuous glucose mentoring. Based on its compatibility with CMOS and MEMS technology, ZnO multilayer structure based SAW glucose biosensor can be integrated on the biosensor chip with readout circuitry and a microfluidic system, and thus the biosensor can be operated with simple and cheap electronic components.

In this work, Mn-ZnO/SiO_2/Si multilayer Love mode SAW biosensor was used to monitor the glucose level for the first time. It was found that the glucose biosensor was highly sensitive, accurate, reversible and stable, which is promising for continuous glucose monitoring.

2. Materials and methods

2.1. Reagents and materials

Acrylic acid, Poly(ethylene glycol) diacrylate (PEGD, 0.02 mol%), isooctyl acrylate, 2,2-Azobis (isobutyronitrile) (AIBN, 0.4 mol%), glucose, glutaric dialdehyde (50 wt%), dimethylaminopropyl-3-ethyl carbodiimide (EDC, 0.46 g/l), N-hydroxysuccinimide (NHS, 0.38 g/L), Glucose oxidase (2 g/L), catalase (0.2 g/L) and bovine serum albumin (BSA, 99%) were purchased from Sigma-Aldrich (Shanghai, China). Bayhydrol 110, an anionic dispersion of an aliphatic polyester urethane resin in water/N-methyl-2-pyrrolidone solution was purchased from Bayer Corp. 0.1 M phosphate buffered solutions (PBS, pH 7.4) containing 10 mM Na_2HPO_4, 10 mM KH_2PO_4 and 2 mM $MgCl_2$ was used throughout the experiment. All the chemicals were of analytical grade or better quality. Human blood serums with glucose concentrations of 4 and 14 mM measured by standard glucose meter were supplied by Nanhua Hospital as the model biological fluid. The human serums were stored at −20 °C and NaN_3 was added as preservative.

2.2. SAW resonators design and SAW glucose sensor fabrication

SiO_2 layers with the optimal thickness of 80 nm were grown on the Si (100) wafer by dry oxidation in an atmospheric furnace at 1025 °C. And then, Mn-doped ZnO film with the concentration of 8 at % was deposited onto SiO_2 layer by direct current reactive magnetron cosputtering. In order to achieve high quality Mn–ZnO films, the sputtering parameters were optimized. The base pressure of the working chamber was lower than 10^{-4} Pa, and the working pressure was a mixture of Ar (0.2 Pa) and O_2 (0.2 Pa). The substrate temperature was 200 °C and the sputtering power was 150 W. The sensitivity of the biosensor and the wave propagation in ZnO/SiO_2/Si structure is related to the thickness of ZnO film (Zhang et al., 2013; Krishnamoorthy et al., 2008). The optimized thickness of 350 nm was determined in this work. The devices were designed to be love mode SAW devices and the displacement of the acoustic wave is in-plane of ZnO film guiding layer, which provides minimal damping of the waves when the film surface is in contact with liquid environments. Thanks to the guided nature of the surface waves, the devices offer the potential of enhanced detection sensitivity. The SAW devices were designed as 2-port resonators which were fabricated via photolithography and the schematic is shown in Fig. 1a. The finger width and spacing of IDTs and reflectors are of 2 μm and the metallization ratio is 0.5. The number of fingers in the input and output IDTs is 30. The number of fingers in the reflectors is 45. The length of the IDTs is 150 μm with an aperture of 130 μm and the length of the reflectors is also 150 μm. The resonator was designed with the SAW wavelength of 8 μm for operation at ~433 MHz which is the industrial, scientific and medical (ISM) license-free frequency bands. The metallizations for the IDTs and reflector plates were 100 nm thick Al films deposited by e-beam evaporation. The central frequency (f_0) of the SAW resonator shown in Fig. 1b is 433.5 MHz, which is coincident to the design one. The SAW resonators with good quality were first subjected to degreasing in pentane, rinsed with acetone and distilled water and dried, then covered with vinyl resin

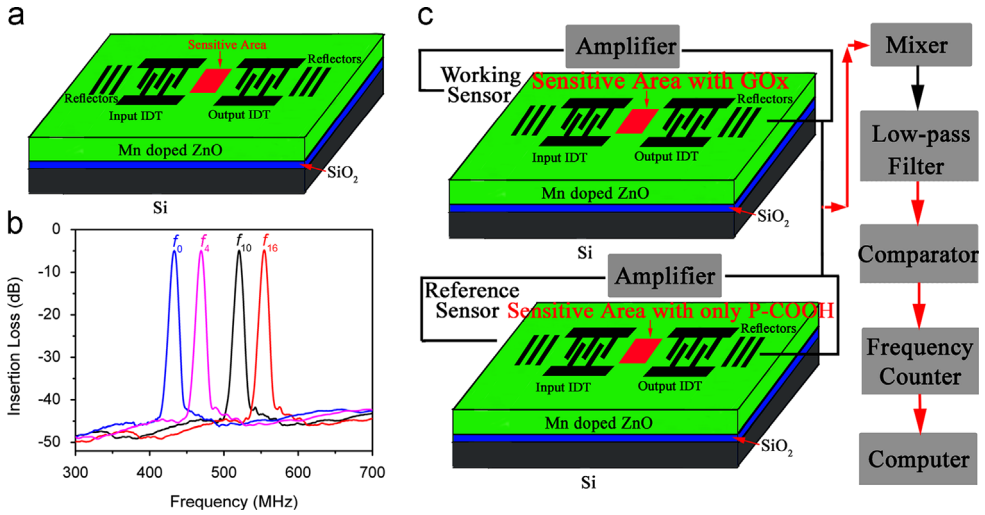

Fig. 1. (a) Schematic diagram of the glucose biosensor based on Mn–ZnO/SiO_2/Si Love-mode SAW resonator. (b) The frequency responses of SAW glucose biosensor. f_0 is the initial resonant frequency of the SAW biosensor without glucose. f_4, f_{10} and f_{16} denote the resonant frequencies of SAW biosensor when the glucose applied on the sensitive area under the concentrations of 4, 10 and 16 mM respectively. and (c) Schematic diagram of the SAW glucose biosensor measurement system.

and mounted with an O-ring on a cell which was designed to expose only the sensitive area.

The key to achieve a stable glucose sensor is the functional immobilization of glucose oxidase (GO*x*) and catalase on the biosensor (Lee et al., 2005; Dai et al., 2009; Wu et al., 2012). Some research works have demonstrated that magnetoelastic sensor coated with a pH-sensitive polymer (P-COOH) immobilized of GO*x* and catalase is successfully used for glucose detection (Cai et al., 2004; Gao et al., 2007). Similarly, in this work, the SAW resonator coated with P-COOH and GO*x* was used to monitor the glucose level. The synthesis process of P-COOH is shown the Supporting Information and the SAW Glucose Sensor fabrication is shown in Fig. S1.

2.3. Experimental setup and measurements

Fig. 1(c) shows the schematic of the SAW glucose biosensor measurement system, which possesses a working sensor cross-correlated with a reference sensor. This is a dual-channel differential measurement system, which can eliminate the false results from the external interference. A mixer is employed to mix the signals from working and reference sensors and outputs their frequency difference. The frequency difference is filtered by a low-pass filter and a comparator is utilized to generate a square wave. Then a frequency counter is used to count frequencies and the data is transported to a computer by RS232 port. In this study, the responses of SAW biosensors system to various glucose level were monitored by recording the differential frequency shifts ($d\Delta f$) between SAW working sensor and reference sensor, which can reflect the changes of mass loading on the sensitive area of SAW biosensor and indicate the changes of glucose concentration. All the measurements were carried out at the same environmental conditions in an incubator chamber with temperature of 25 °C.

High-resolution transmission electron microscopy ((HRTEM), JEM2011, Hitachi, Japan) was used to study the structural characteristics of Mn–ZnO films. The functional immobilization of enzyme on the biosensor was observed using a LEO1530 field emission scanning electron microscope (SEM). Atomic force microscopy (AFM) was employed to characterize the functionalization of SAW glucose biosensor. X-ray photoelectron spectroscopy (XPS) was used to characterize the chemical state and composition of Mn-doped ZnO films. The pH value around the sensitive area of the working sensor was measured by pH measuring instrument (Orion STAR A211).

3. Results and discussions

3.1. Characterization of Mn-doped ZnO piezoelectric thin film

It is known that, the sensitivity of the SAW biosensor strongly depends on the microstructure and piezoelectric property of the piezoelectric material (Fu et al., 2010). Our previous works have demonstrated that the piezoelectric property of ZnO films can be greatly enhanced via Mn-doping. The piezoelectric coefficient d_{33} was enhanced from undoped ZnO of 12.1 pC/N to ~8% Mn-doped ZnO with maximum value of ~86 pC/N (Luo et al., 2010). Therefore, 8% Mn-doped ZnO film was used as the piezoelectric material in this work. For the successful application of ZnO film in SAW biosensing, ZnO film should possess high crystal quality with low defects and high uniformity in microstructure and thickness.

The HRTEM was used to investigate the microstructure of Mn–ZnO films. Fig. 2(a) exhibits a representative low magnification TEM image of Mn–ZnO film, which is taken from a cross-sectional specimen. Columnar grains that penetrate through the film can be clearly observed, indicating the strong *c*-axis preferred orientation of Mn–ZnO films. A relatively flat surface and a uniform thickness of ~350 nm are also revealed. Fig. 2(b) shows that the film has a nanoscale polycrystalline structure. A typical (002) crystal grain is marked by two black arrows which shows

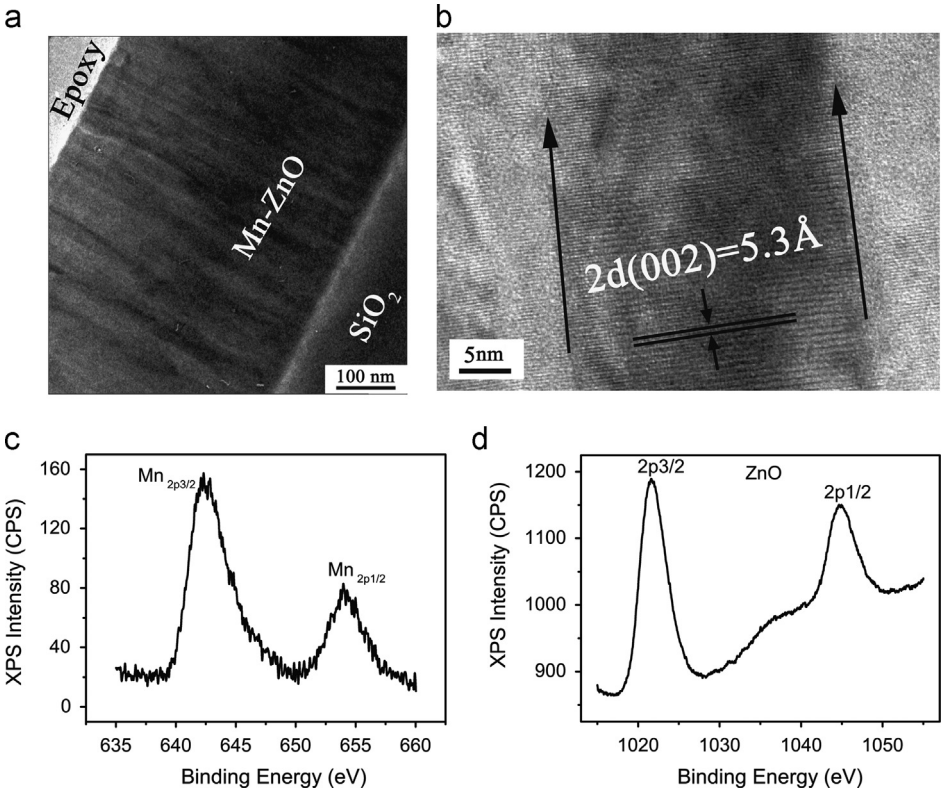

Fig. 2. (a) A low magnification TEM image of the cross-sectional specimen of Mn–ZnO films on SiO_2. (b) A HRTEM image of Mn–ZnO films. (c) Mn 2p XPS spectra of the åMn-doped ZnO film. and (d) ZnO 2p XPS spectra of the Mn-doped ZnO film.

the growth direction of the film. The area between the two black arrows is a ~20 nm diameter columnar grain. Herein, the deposited Mn–ZnO film is of high crystal quality with low defects, which is promising for SAW bio-sensing applications. XPS spectra taken from the Mn and Zn regions of Mn-doped ZnO film were shown in Fig. 2(c) and (d), respectively. It is shown that the Mn $2p_{3/2}$ and Mn $2p_{1/2}$ in the film are located at about 642.4 and 654.1 eV, respectively, which are very close to that of Mn^{4+}. The peaks at about 1021.8 and 1044.7 eV (Fig. 2(d)) are attributed to $Zn_{2p3/2}$ and $Zn_{2p1/2}$, which agrees well with the data for Zn_{2p} in ZnO.

3.2. Morphological and binding properties of enzyme on the sensitive area

The functional immobilization of enzyme on the biosensor is crucial for SAW bio-sensing. SEM and AFM were employed to characterize the functional immobilization of enzyme on the sensitive area of SAW biosensor. Fig. 3(a) shows the SEM image of the bare cleaned and fresh sensitive area. Before functionalization, the bare sensitive area is pretty smooth with low roughness, which is satisfied for SAW bio-sensing applications. Fig. 3(b) shows the SEM images of GO*x* functionalized sensitive area. It is found that some dots with a similar diameter around 50 nm are distributed on the surface. It is suggested that these dots could be the immobilized enzyme. AFM was used to further characterize the surface morphology and binding properties of enzyme on the sensitive area. The AFM scans of a larger area show the similar dots distribution on the sensitive area immobilized with enzyme (Fig. 3(c)). Fig. 3(d) shows the height of the dots is approximately 10–20 nm. The large and similar size of the dots on the sensitive area shows that the covalent functional immobilization of enzyme is efficient. The covalent immobilization of enzyme is much stable than physical absorption due to the much stronger forces between enzyme and sensitive surface, which is important for sensitive and stable SAW bio-sensing (Krishnamoorthy et al., 2006).

3.3. Detection of glucose

After the functionalization of the SAW glucose biosensor, the sensors were activated in PBS (0.1 M pH 7.4) to wet the polymer before measurement, and then immersed in the testing solution. In the presence of glucose, the following reactions occur on the glucose biosensor (Gao et al., 2007; Cai et al., 2004; Guerrieri et al., 1998):

$$\text{Glucose} + O_2 + H_2O \overset{GOx}{\Longrightarrow} \text{gluconic acid} + H_2O_2 \quad (1)$$

$$H_2O_2 \overset{catalase}{\Longrightarrow} 1/2O_2 + H_2O \quad (2)$$

Resulting in the overall enzyme reaction:

$$\text{Glucose} + 1/2O_2 \overset{GOx+catalase}{\Longrightarrow} \text{gluconic acid} \quad (3)$$

The dissociation of gluconic acid produces H^+, resulting in a decreasing pH that is detected by P-COOH. In response to the pH decrease, the P-COOH shrinks, reducing the mass loading on the SAW biosensor. The SAW resonator is sensitive to the mass loading on the path of the traveling wave (Gronewold, 2007; Laenge et al., 2008; Voiculescu and Nordin, 2012). With the mass loading decreases, the resonant frequency of SAW biosensor increases. As shown in Fig. 1(b), when the glucose with the concentration of 4, 10 and 16 mM applied on SAW biosensor, the resonant frequencies shift to f_4, f_{10} and f_{16}, respectively. The resonant frequency shifts gradually, reflecting the change of mass loading, and in turn monitoring the glucose concentration change in the measurement system.

3.4. Sensitivity characterization of SAW glucose biosensor

Under normal physiological conditions, serum glucose concentration is around 3.8–6.1 mM, while the glucose level of diabetic could decrease to 2 mM at midnight or under excessive injection of insulin, and could reach as high as 16 mM when hyperglycemia happens. Therefore, we calibrated our sensor using glucose concentrations ranging from 2 to 16 mM with the spacing of 2 mM, meanwhile, 0.15 M NaCl was added to imitate physiological conditions. The time-dependent response profiles of the SAW glucose sensor in physiological solutions with glucose concentrations ranging from 2 to 16 mM are shown in Fig. 4(a). The instantaneous shifts in the differential frequency occurred by the addition of glucose and rapidly reached stationary levels within 200 s.

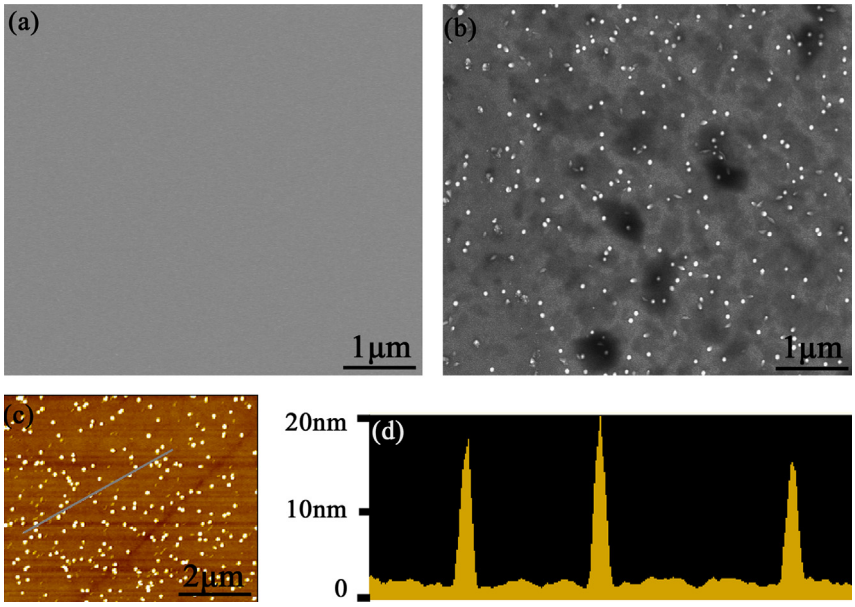

Fig. 3. Characterization of functional immobilization of enzyme on the sensitive area. (a) SEM image of the bare cleaned and fresh sensitive area. (b) SEM image of the sensitive area immobilized with enzyme. (c) AFM scans of the sensitive area immobilized with enzyme and (d) the height of the three dots crossed by the oblique straight line in (c).

After the $d\Delta f$ of the glucose biosensor system was stable, a pH measuring instrument was used to detect the pH value around the sensitive area of the working sensor and the pH value with respect to glucose concentration is shown in Fig. 4(b). The pH value decreases with increasing of glucose concentration, which indicates the increasing of gluconic acid content. The statistical total $d\Delta f$ of SAW in response to glucose concentrations are shown in Fig. 4(b). It is known that the frequency shift Δf due to mass loading change Δm of a SAW device is described by (Buttry and Ward, 1992)

$$\Delta f = k\frac{\Delta m {f_0}^2}{A} \tag{4}$$

where k, f_0, and A are the basal coefficient of the sensitive material, the intrinsic resonant frequency of the SAW biosensor and the sensitive area. The increase of glucose concentration enhances the reaction of glucose to gluconic acid and produces more H^+, resulting in a decreasing pH and the shrinking of P-COOH. As a result, the mass loading on the SAW biosensor decreases and the resonant frequency of SAW biosensor shifts to a higher one. Plotting the $d\Delta f$ against the glucose concentration, a calibration curve is obtained with a regression coefficient of 0.991 (Fig. 4(b)). It is indicated that a well linear response can be obtained in a concentration-dependent manner in the concentration ranging from 2 to 16 mM. The sensitivity of this glucose biosensor can be obtained by the slope of the calibration curve, and the obtained 7.184 MHz/mM does show it. For SAW biosensor measurement, the noise can be smaller than ~300 Hz from the blank response. Defining the detection limit as the concentration that can be detected at ten times the noise level, the detection limit is lower than 4.2×10^{-4} mM.

3.5. Anti-interference features and reversibility characterization

The mechanism of our SAW glucose biosensor is based on the mass load change of the P-COOH, which is resulted from the pH changing of the testing solution. However, the pH changing in the blood is complicated. Besides the oxidation of glucose, the local pH changing can also be contributed by ascorbic acid, lactic acid and uric acid. Therefore, the anti-interference ability of the SAW glucose biosensor to ascorbic acid, lactic acid and uric acid was examined. Fig. 4(c) shows the selective response of the biosensor to glucose and its interferent ascorbic acid, lactic acid and uric acid. It was found that an instantaneous shift in the frequency difference occurred by the injection of 2 mM glucose and rapidly reached a stationary level. Control experiments results showed that the $d\Delta f$ for the glucose interferent is very small at the beginning and almost no differential SAW frequency shift can be observed with the time go on. Although the working SAW sensor can be influenced by ascorbic acid, lactic acid and uric acid, this effect is the same to the reference SAW sensor, and thus almost no differential SAW frequency shift can be observed by the SAW glucose biosensor measurement system through dual-channel differential testing. Thus, the anti-interference ability of the SAW glucose biosensor measurement system is good and the SAW glucose biosensor system in this work is highly specific to glucose. The high specificity of the glucose sensor is ascribed to the specificity of the enzymatic reaction (Dai et al., 2009; He et al., 2012).

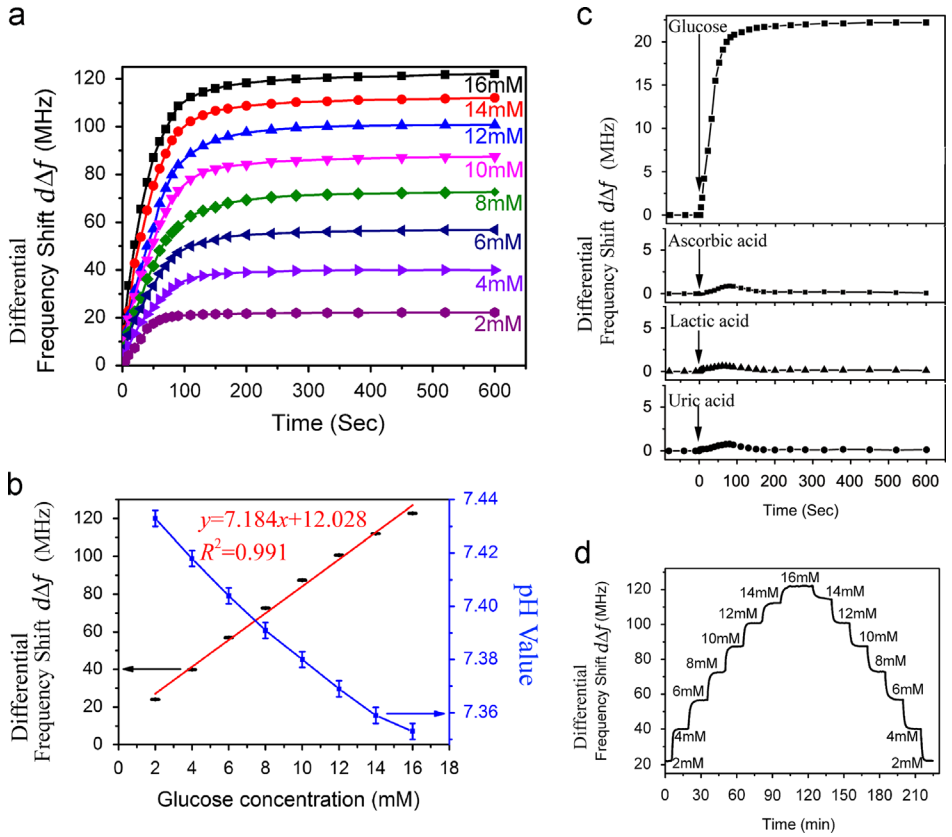

Fig. 4. (a) Time-dependent differential responses profiles from the mixer of working biosensor and reference one to various glucose concentrations. (b) The $d\Delta f$ of SAW biosensor system as functions of glucose concentration. The red straight line is the calibration curve of the biosensor to glucose concentration. The blue line is the corresponding pH value around the sensitive area when the $d\Delta f$ is stable. (c) The $d\Delta f$ of the SAW glucose biosensor system when glucose, ascorbic acid, lactic acid, and uric acid were applied on it. (d) The $d\Delta f$ of the SAW glucose biosensor system to stepwise increasing and decreasing glucose concentrations (2–4–6–8–10–12–14–16 mM) in physiological solution. The standard deviations in the measurement are no more than 50 kHz. (For interpretation of the references to color in this figure legend, the reader is referred to the web version of this article.)

The reversibility of the biosensor is also important for its medical application. Therefore, continuous measurement of glucose concentrations at the stepwise increasing levels (2–4–6–8–10–12–14–16 mM) are performed, followed by similar decreasing levels (16–14–12–10–8–6–4–2 mM), and the corresponding $d\Delta f$ is shown in Fig. 4(d). The $d\Delta f$ characterizing a glucose level is the same after increasing or decreasing the glucose concentration. The reversibility of $d\Delta f$ is expected since the mass load of the P-COOH is reversible with glucose concentration. Hereby, the fabricated SAW glucose biosensor was highly reversible when responsed to stepwise increasing and decreasing glucose concentrations in physiological solution.

3.6. Reproducibility and stability characterization

The reproducibility and stability of the biosensor are very important for glucose monitoring. Therefore, two solutions with extreme glucose concentration, namely 2 and 16 mM were alternately added on the glucose sensor. As shown in Fig. 5(a), 11 full cycles performed without interruption during 10 h demonstrated a high reproducibility and stability of the sensor. The $d\Delta f$ difference between 2 and 16 mM was constant throughout the measurement. For each equilibrium value of glucose concentration, more than 100 measurements were averaged, leading to a standard deviation of 25 kHz. The glucose sensitivity was 7.184 MHz/mM, which combined with a 95% confidence interval of 50 kHz (2σ), results showed that the accuracy of the SAW glucose biosensor was 6.96×10^{-3} mM. This value is more accurate than the 1 mg/dl (5.6×10^{-2} mM) resolution of conventional glucose meters (Boss et. al., 2011; Laenge et al., 2008). It was found that the SAW biosensor resolution was accurate enough for tracking the deviation of glucose level. Moreover, no decrease in the sensor sensitivity was observed, demonstrating a high stability.

3.7. In vitro determination of glucose in human serum

Herein, the SAW glucose biosensor showed fast response, high specificity, sensitivity and stability for glucose monitoring in physiological solutions. However, when it is used to monitor the glucose in the blood, some components in the blood could interfere with the sensitive solutions. Thereby, the SAW glucose biosensor system was also evaluated using human blood serum as a model biological fluid. Two kind of human blood serum with glucose concentrations of 4 and 14 mM were alternately added on the glucose sensor and 12 full cycles of $d\Delta f$ are shown in the inset of Fig. 5(b). The $d\Delta f$ for 4 and 14 mM serum are ~38.3 MHz and ~107.3 MHz, respectively. The diffusion of glucose to the sensor and the gluconic acid to P-COOH were well described by the exponential model, which tended to show that two diffusion processes were governing the sensor kinetics. Therefore, the response time was determined by fitting the sensor response to multiple glucose variations (more than 100 measurements) using an exponential relationship. The time response of the sensor (time to reach 98% of the equilibrium value) was 4.6 ± 0.4 min when increasing glucose concentrations, and 7.1 ± 0.6 min when decreasing. As for medical applications, the required time response of the glucose measurement should be less than 10 min (Boss et al., 2011). Therefore, the glucose biosensor in this work is satisfied to the fast response requirement for medical application. The longer time constant related to decreasing glucose concentrations could be explained by a smaller recover speed of the pH value and P-COOH in the solution.

The long-term stability characterization of the SAW glucose biosensor was performed by testing its responses to serum with glucose concentrations of 4 mM and 14 mM every day for more than 6 weeks. As shown in Fig. 5(b), the $d\Delta f$ for 4 mM and 14 mM serum are ~38.3 MHz and ~107.3 MHz respectively on the first day, and the responses of this biosensor to glucose is stable during the subsequent 32 days. The $d\Delta f$ decrease to ~37.2 MHz and

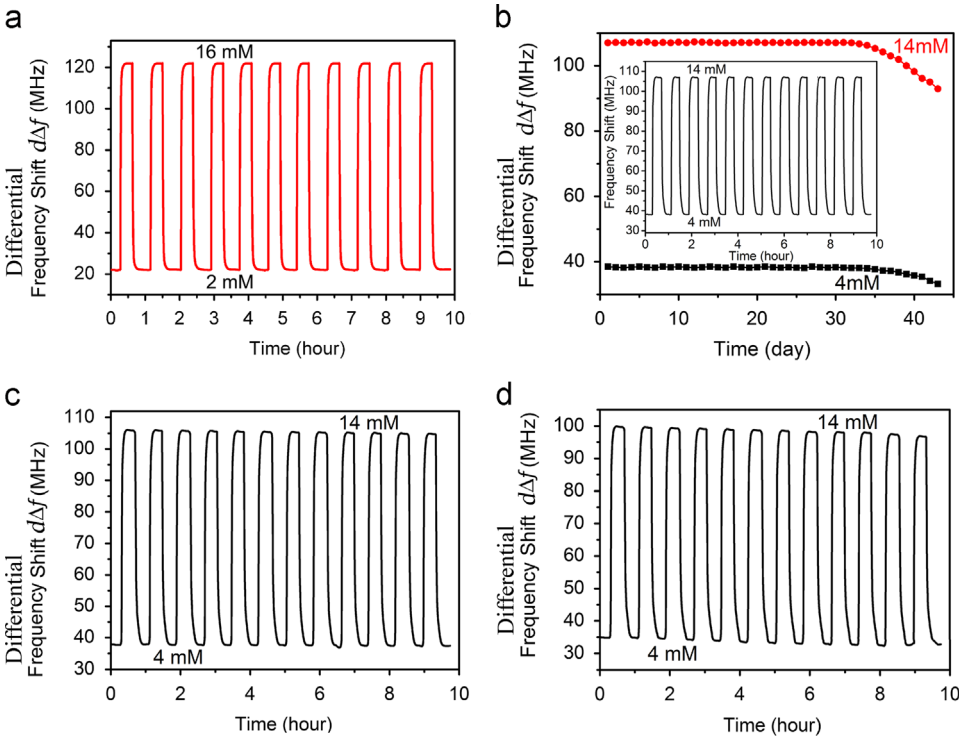

Fig. 5. The reproducibility and long-term stability characterization of the SAW glucose biosensor. (a) The $d\Delta f$ response to 11 full cycles of glucose concentrations (2 and 16 mM) in physiological solution. (b) The $d\Delta f$ response to human blood serum with glucose concentrations of 4 and14 mM for 43 days. The 12 full cycles of $d\Delta f$ profile to human blood serum with concentrations of 4 and 14 mM on the three special days, the inset of (b) is on the first day, (c) on the 35th day, and (d) on the 40th day. åThe standard deviations in the measurement are no more than 60 kHz.

~105.1 MHz respectively for 4 mM and 14 mM serum on the 35th day (Fig. 5(c)). On the 40th day (Fig. 5(d)), the $d\Delta f$ of SAW biosensor system to 4 mM and 14 mM serum decreases to ~32.7 MHz and ~96.2 MHz respectively, which are still more than 85% of the initial values and the sensitivity of the sensor in serum is still high enough for glucose monitoring. It is suggested that the decrease of glucose biosensor sensitivity is due to frequent measurement, exposure to ambient and the gradual activity loss of GO*x* and catalase. The stability of the glucose biosensor would be higher when it is sealed. However, for long-term monitoring application, the function stability of the SAW glucose biosensor is still a big challenge, which will be the focus of our near future research works.

4. Conclusions

This work developed a highly sensitive Love mode Mn–ZnO/SiO_2/Si multilayer structure SAW biosensor targeting continuous glucose monitoring for the first time. The glucose oxidase was well immobilized onto a P-COOH attached on Mn–ZnO SAW biosensor for glucose detection. The anti-interference ability of the fabricated SAW glucose biosensor to ascorbic acid, lactic acid and uric acid was good. The glucose biosensor demonstrated highly sensitivity, accuracy, reversibility and long-term stable, which is promising for glucose monitoring. Owing to the passive, wireless and telemetering features of SAW biosensor, our fabricated SAW glucose biosensor is promising for glucose monitoring in vivo, and the implantation study of our SAW glucose biosensor will be the focus of our near future research works.

Acknowledgments

This work was supported by the National Hi-tech (R&D) project of China (Grant no. 2009AA034001), the National Natural Science Foundation of China (Grants no. 11174208), the Basical Research Program of Shenzhen (Grants nos. JC201104210094A and JCYJ20120817163755062) and the Natural Science Foundation of SZU (Grants no. 801 00035699).

Appendix A. Supporting information

Supplementary data associated with this article can be found in the online version at http://dx.doi.org/10.1016/j.bios.2013.05.021.

References

Arya, S.K., Saha, S., Ramirez-Vick, J.E., Gupta, V., Bhansali, S., Singh, S.P., 2012. Analytica Chimica Acta 737, 1–21.
Atanasov, P., Yang, S., Salehi, C., Ghindilis, A.L., Wilkins, E., Schade, D., 1997. Biosensors and Bioelectronics 12, 669–680.
Boss, C., Meurville, E., Sallese, J.-M., Ryser, P., 2011. Biosensors and Bioelectronics 30, 223–228.
Buttry, D.A., Ward, M.D., 1992. Chemical Reviews 92, 1355.
Cai, Q.Y., Zeng, K.F., Ruan, C.M., Desai, T.A., Grimes, C.A., 2004. Analytical Chemistry 76, 4038–4043.
Dai, Z., Shao, G., Hong, J., Bao, J., Shen, J., 2009. Biosensors and Bioelectronics 24, 1286–1291.
Di Pietrantonio, F., Cannata, D., Benetti, M., Verona, E., Varriale, A., Staiano, M., D'Auria, S., 2013. Biosensors and Bioelectronics 41, 328–334.
Fu, Y.Q., Luo, J.K., Du, X.Y., Flewitt, A.J., Li, Y., Markx, G.H., Walton, A.J., Milne, W.I., 2010. Sensors and Actuators B 143, 606–619.
Gao, X.J., Yang, W.Y., Pang, P.F., Liao, S.T., Cai, QY., Zeng, K.F., Grimes, C.A., 2007. Sensors and Actuators B 128, 161–167.
Gronewold, T.M.A., 2007. Analytica Chimica Acta 603 (2), 119–128.
Guerrieri, A., De Benedetto, G.E., Palmisano, F., Zambonin, P.G., 1998. Biosensors and Bioelectronics 13, 103–112.
He, H.L., Xu, X.L., Wu, H.X., Jin, Y.D., 2012. Advanced Materials 24, 1736–1740.
Jung, A., Gronewold, T.M.A., Tewes, M., Quandt, E., Berlin, P., 2007. Sensors and Actuators B 124, 46–52.
Katardjiev, I., Yantchev, V., 2012. Vacuum 86, 520–531.
Klueh, U., Dorsky, D.I., Kreutzer, D.L., 2005. Biomaterials 26, 1155–1163.
Kottmann, J., Rey, J.M., Luginbuehl, J., Reichmann, E., Sigrist, M.W., 2012. Biomedical Optics Express 3, 667–680.
Krishnamoorthy, S., Bei, T., Zoumakis, E., Chrousos, G.P., Iliadis, A.A., 2006. Biosensors and Bioelectronics 22, 707–714.
Krishnamoorthy, S., Iliadis, A.A., Bei, T., Chrousos, G.P., 2008. Biosensors and Bioelectronics 24, 313–318.
Laenge, K., Rapp, B.E., Rapp, M., 2008. Analytical and Bioanalytical Chemistry 391, 1509–1519.
Lee, D., Lee, J., Kim, J., Na, H.B., Kim, B., Shin, C.H., Kwak, J.H., Dohnalkova, A., Grate, J. W., Hyeon, T., Kim, H.S., 2005. Advanced Materials 17, 2828–2833.
Lee, K., Wang, W., Kim, T., Yang, S., 2007. Journal of Micromechanics and Microengineering 17, 515–523.
Luo, J.T., Zhu, X.Y., Chen, G., Zeng, F., Pan, F., 2010. Physca Status Solidi (R) 2010 (4), 209–211.
Pohl, A., 2000. IEEE Transactions on Ultrasonics Ferroelectrics 47, 317–332.
Rocha-Gaso, M.I., March-Iborra, C., Montoya-Baides, A., Arnau-Vives, A., 2009. Sensors 9, 5740–5769.
Shibata, H., Heo, Y.J., Okitsu, T., Matsunaga, Y., Kawanishi, T., Takeuchi, S., 2010. Proceedings of the National Academy of Sciences USA 107, 17894–17898.
Vashist, S.K., 2012. Analytica Chimica Acta 750, 16–27.
Voiculescu, I., Nordin, A.N., 2012. Biosensors and Bioelectronics 33, 1–9.
Wang, N., Burugapalli, K., Song, W., Halls, J., Moussy, F., Ray, A., Zheng, Y., 2013. Biomaterials 34, 889–901.
WHO, 2013. World Health Organization. ⟨http://www.who.int/mediacentre/factsheets/fs312/en/⟩.
Wu, C., Du, L., Wang, D., Zhao, L., Wang, P., 2012. Biosensors and Bioelectronics 31, 44–48.
Yan, X.F., Li, D.M., Hou, C.C., Wang, X., Zhou, W., Liu, M., Ye, T.C., 2012. Sensors and Actuators B 161, 329–333.
Zhang, Z.W., Wen, Z.Y., Wang, C.M., 2013. Ultrasonics 53, 363–368.